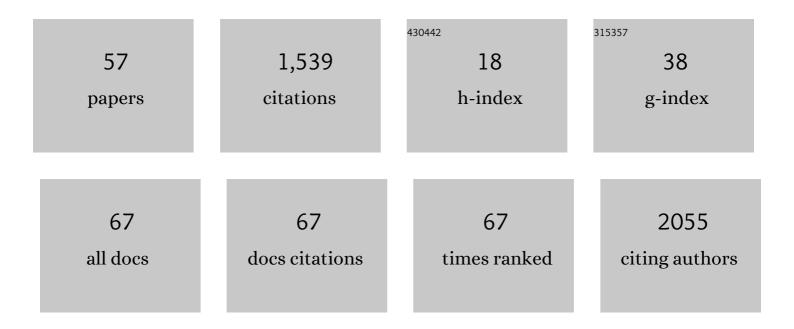
Ting-Yim Lee

List of Publications by Year in descending order

Source: https://exaly.com/author-pdf/1247557/publications.pdf Version: 2024-02-01



TINC-YIM LEE

#	Article	IF	CITATIONS
1	An Adiabatic Approximation to the Tissue Homogeneity Model for Water Exchange in the Brain: I. Theoretical Derivation. Journal of Cerebral Blood Flow and Metabolism, 1998, 18, 1365-1377.	2.4	373
2	Hemorrhagic Transformation of Ischemic Stroke: Prediction with CT Perfusion. Radiology, 2009, 250, 867-877.	3.6	152
3	Simultaneous MRI measurement of blood flow, blood volume, and capillary permeability in mammary tumors using two different contrast agents. Journal of Magnetic Resonance Imaging, 2000, 12, 991-1003.	1.9	128
4	Impact of new technologies on dose reduction in CT. European Journal of Radiology, 2010, 76, 28-35.	1.2	97
5	Correlation between Hepatic Tumor Blood Flow and Glucose Utilization in a Rabbit Liver Tumor Model. Radiology, 2006, 239, 740-750.	3.6	60
6	Non-invasive assessment of functionally relevant coronary artery stenoses with quantitative CT perfusion: preliminary clinical experiences. European Radiology, 2012, 22, 39-50.	2.3	54
7	Assessment of a multi-layered diffuse correlation spectroscopy method for monitoring cerebral blood flow in adults. Biomedical Optics Express, 2016, 7, 3659.	1.5	47
8	Quantitative myocardial perfusion measurement using CT Perfusion: a validation study in a porcine model of reperfused acute myocardial infarction. International Journal of Cardiovascular Imaging, 2012, 28, 1237-1248.	0.7	43
9	Hepatic perfusion in a tumor model using DCE-CT: an accuracy and precision study. Physics in Medicine and Biology, 2008, 53, 4249-4267.	1.6	40
10	Dynamic contrast enhanced CT aiding gross tumor volume delineation of liver tumors: An interobserver variability study. Radiotherapy and Oncology, 2014, 111, 153-157.	0.3	34
11	Assessment of the best flow model to characterize diffuse correlation spectroscopy data acquired directly on the brain. Biomedical Optics Express, 2015, 6, 4288.	1.5	34
12	Quantitative myocardial CT perfusion: a pictorial review and the current state of technology development. Journal of Cardiovascular Computed Tomography, 2011, 5, 467-481.	0.7	32
13	Low dose CT perfusion in acute ischemic stroke. Neuroradiology, 2014, 56, 1055-1062.	1.1	32
14	Low Birth Weight Male Guinea Pig Offspring Display Increased Visceral Adiposity in Early Adulthood. PLoS ONE, 2014, 9, e98433.	1.1	30
15	Quantifying cerebral blood flow in an adult pig ischemia model by a depth-resolved dynamic contrast-enhanced optical method. NeuroImage, 2014, 94, 303-311.	2.1	27
16	Quantification of blood-brain barrier permeability by dynamic contrast-enhanced NIRS. Scientific Reports, 2017, 7, 1702.	1.6	26
17	Improved light collection and wavelet de-noising enable quantification of cerebral blood flow and oxygen metabolism by a low-cost, off-the-shelf spectrometer. Journal of Biomedical Optics, 2014, 19, 057007.	1.4	22
18	Dynamic perfusion CT in brain tumors. European Journal of Radiology, 2015, 84, 2386-2392.	1.2	22

TING-YIM LEE

#	Article	IF	CITATIONS
19	CT Perfusion as an Early Biomarker of Treatment Efficacy in Advanced Ovarian Cancer: An ACRIN and GOG Study. Clinical Cancer Research, 2017, 23, 3684-3691.	3.2	20
20	The Effect of Scan Duration on the Measurement of Perfusion Parameters in CT Perfusion Studies ofÂBrain Tumors. Academic Radiology, 2013, 20, 59-65.	1.3	18
21	Technical Note: Evaluation of a 160-mm/256-row CT scanner for whole-heart quantitative myocardial perfusion imaging. Medical Physics, 2016, 43, 4821-4832.	1.6	18
22	Monitoring brain temperature by time-resolved near-infrared spectroscopy: pilot study. Journal of Biomedical Optics, 2014, 19, 057005.	1.4	15
23	Subcutaneous administration of nimodipine improves bioavailability in rabbits. Journal of Neuroscience Methods, 2004, 139, 195-201.	1.3	14
24	Prediction and Reduction of Motion Artifacts in Free-Breathing Dynamic Contrast Enhanced CT Perfusion Imaging of Primary and Metastatic Intrahepatic Tumors. Academic Radiology, 2013, 20, 414-422.	1.3	13
25	Improving Quantitative CT Perfusion Parameter Measurements Using Principal Component Analysis. Academic Radiology, 2014, 21, 624-632.	1.3	11
26	Non-invasive monitoring of brain temperature by near-infrared spectroscopy. Temperature, 2015, 2, 31-32.	1.7	10
27	Functional CT assessment of extravascular contrast distribution volume and myocardial perfusion in acute myocardial infarction. International Journal of Cardiology, 2018, 266, 15-23.	0.8	10
28	Assessment of tumour response after stereotactic ablative radiation therapy for lung cancer: A prospective quantitative hybrid 18 Fâ€fluorodeoxyglucoseâ€positron emission tomography and CT perfusion study. Journal of Medical Imaging and Radiation Oncology, 2019, 63, 94-101.	0.9	10
29	Characterization of 5-(2-18F-fluoroethoxy)-L-tryptophan for PET imaging of the pancreas. F1000Research, 2016, 5, 1851.	0.8	10
30	Assessment of contrast enhanced respiration managed cone-beam CT for image guided radiotherapy of intrahepatic tumors. Medical Physics, 2014, 41, 051905.	1.6	9
31	Western diet consumption through early life induces microvesicular hepatic steatosis in association with an altered metabolome in low birth weight Guinea pigs. Journal of Nutritional Biochemistry, 2019, 67, 219-233.	1.9	9
32	High-Frequency Ultrasound to Grade Disease Progression in Murine Models of Duchenne Muscular Dystrophy. Journal of Ultrasound in Medicine, 2009, 28, 707-716.	0.8	8
33	Anatomy-based algorithm for automatic segmentation of human diaphragm in noncontrast computed tomography images. Journal of Medical Imaging, 2016, 3, 046004.	0.8	8
34	Rapid and selective brain cooling method using vortex tube: A feasibility study. American Journal of Emergency Medicine, 2016, 34, 887-894.	0.7	8
35	Relationship of computed tomography perfusion and positron emission tomography to tumour progression in malignant glioma. Journal of Medical Radiation Sciences, 2014, 61, 4-13.	0.8	7
36	Coupling of cerebral blood flow and oxygen consumption during hypothermia in newborn piglets as measured by time-resolved near-infrared spectroscopy: a pilot study. Neurophotonics, 2015, 2, 035006.	1.7	7

TING-YIM LEE

#	Article	IF	CITATIONS
37	Joint blood flow is more sensitive to inflammatory arthritis than oxyhemoglobin, deoxyhemoglobin, and oxygen saturation. Biomedical Optics Express, 2016, 7, 3843.	1.5	7
38	Predicting pathological complete response (pCR) after stereotactic ablative radiation therapy (SABR) of lung cancer using quantitative dynamic [18F]FDG PET and CT perfusion: a prospective exploratory clinical study. Radiation Oncology, 2021, 16, 11.	1.2	7
39	Multimodality In Vivo Imaging of Perfusion and Glycolysis in a Rat Model of C6 Glioma. Molecular Imaging and Biology, 2021, 23, 516-526.	1.3	7
40	Evaluation of Four-Dimensional Computed Tomography as a Technique for Quantifying Carpal Motion. Journal of Biomechanical Engineering, 2021, 143, .	0.6	7
41	Assessment of intratumor hypoxia by integrated 18F-FDG PET / perfusion CT in a liver tumor model. PLoS ONE, 2017, 12, e0173016.	1.1	7
42	Detecting Degenerative Changes in Myotonic Murine Models of Duchenne Muscular Dystrophy Using High-Frequency Ultrasound. Journal of Ultrasound in Medicine, 2010, 29, 367-375.	0.8	6
43	Prospective Multicenter Study of Changes in MTT after Aneurysmal SAH and Relationship to Delayed Cerebral Ischemia in Patients with Good- and Poor-Grade Admission Status. American Journal of Neuroradiology, 2018, 39, 2027-2033.	1.2	6
44	CT Perfusion Techniques and Applications in Stroke and Cancer. , 2020, , 347-365.		6
45	Blood–brain barrier permeability in survivors of immune-mediated thrombotic thrombocytopenic purpura: a pilot study. Blood Advances, 2021, 5, 4211-4218.	2.5	4
46	Plasma radio-metabolite analysis of PET tracers for dynamic PET imaging: TLC and autoradiography. EJNMMI Research, 2020, 10, 141.	1.1	4
47	Quantitative low-dose rest and stress CT myocardial perfusion imaging with a whole-heart coverage scanner improves functional assessment of coronary artery disease. IJC Heart and Vasculature, 2019, 24, 100381.	0.6	3
48	Kinetic analysis of dominant intraprostatic lesion of prostate cancer using quantitative dynamic [18F]DCFPyL-PET: comparison to [18F]fluorocholine-PET. EJNMMI Research, 2021, 11, 2.	1.1	3
49	Technical Note: Volumetric computed tomography for radiotherapy simulation and treatment planning. Journal of Applied Clinical Medical Physics, 2021, 22, 295-302.	0.8	3
50	CT Perfusion Imaging as an Early Biomarker of Differential Response to Stereotactic Radiosurgery in C6 Rat Gliomas. PLoS ONE, 2014, 9, e109781.	1.1	3
51	Simultaneous MRI measurement of blood flow, blood volume, and capillary permeability in mammary tumors using two different contrast agents. , 2000, 12, 991.		2
52	Short-duration dynamic [18F]DCFPyL PET and CT perfusion imaging to localize dominant intraprostatic lesions in prostate cancer: validation against digital histopathology and comparison to [18F]DCFPyL PET/MR at 120 minutes. EJNMMI Research, 2021, 11, 107.	1.1	2
53	Low-dose CT Perfusion with Sparse-view Filtered Back Projection in Acute Ischemic Stroke. Academic Radiology, 2022, 29, 1502-1511.	1.3	1
54	Imaging Biomarkers in Prostate Stereotactic Body Radiotherapy: A Review and Clinical Trial Protocol. Frontiers in Oncology, 2022, 12, 863848.	1.3	1

TING-YIM LEE

#	Article	IF	CITATIONS
55	Effect of Cardiac Phase on Cardiac Output Index Derived from Dynamic CT Myocardial Perfusion Imaging. Tomography, 2022, 8, 1129-1140.	0.8	1
56	4D CT for Respiratory Gated Attenuation Corrections in Canine Cardiac PET Imaging. , 0, , .		0
57	Contrast Media in Computed Tomography Imaging. , 2013, , 25-67.		0